Eur J Appl Physiol (2003) 90: 305–316
DOI 10.1007/s00421-003-0915-2

ORIGINAL ARTICLE

M. Meyer · O. Stiedl

Self-affine fractal variability of human heartbeat interval dynamics in health and disease

Accepted: 19 June 2003 / Published online: 27 August 2003

Abstract The complexity of the cardiac rhythm is demonstrated to exhibit self-affine multifractal variability. The dynamics of heartbeat interval time series was analyzed by application of the multifractal formalism based on the Cramèr theory of large deviations. The continuous multifractal large deviation spectrum uncovers the nonlinear fractal properties in the dynamics of heart rate and presents a useful diagnostic framework for discrimination and classification of patients with cardiac disease, e.g., congestive heart failure. The characteristic multifractal pattern in heart transplant recipients or chronic heart disease highlights the importance of neuroautonomic control mechanisms regulating the fractal dynamics of the cardiac rhythm.

Keywords Cardiac disease · Heart rate variability · Large deviation spectrum · Multifractals

Introduction

The beat-to-beat variation in the heart rate of humans and other mammals is generated by a complex process and displays inhomogeneous, nonstationary extremely irregular temporal organization. The physiological mechanisms of cardiac control expected to result from both intrinsic and extrinsic factors operating at different time scales or resolution have not been identified clearly. A variety of mathematical methods have been developed to characterize complex patterns in physiological time series. These methods include classical linear stochastic techniques such as the mean and standard deviation, as well as novel methods derived from nonlinear systems theory including fractal dimension, scaling coefficients and multifractal spectra. The various ways in which these measures may be applied to analyze physiological dynamics are briefly reviewed with emphasis on techniques of assessment and modeling of the multifractal properties of cardiac time series.

In this article we will first summarize standard methods of time series analysis pointing at the pitfalls inherent in the application to a stream of heartbeat interval data. Then some techniques in which concepts from nonlinear systems dynamics have been applied will be addressed. These include unifractal and multifractal approaches of analysis. Finally, multifractal modeling of cardiac time series complements this overview. However, since an extensive allusion to methods of nonlinear time series analysis is presented in several recent general textbooks (Bassingthwaighte et al. 1994; Kaplan and Glass 1995; Abarbanel 1996; Kantz and Schreiber 1997; Mandelbrot 1999; West 1999; Bunde et al. 2002; Doukhan et al. 2003), we will not attempt a comprehensive review. In addition, the choice of methods is not exclusively based on objective criteria, rather there is a strong bias towards methods that we have found either conceptually interesting or useful in practical work, or both.

Assessment of heart rate dynamics

Standard methods of time series analysis – when the mean is meaningless

In research, quantitative analysis of physiological signals typically starts (and often ends) with an analysis of the mean and standard deviation. However it does not seem to be recognized that the most commonly used linear-stochastic statistical procedures provide an adequate characterization of the data *only if the data have some very specific mathematical properties*.

Dedicated to Paolo Cerretelli on the occasion of his 70th birthday anniversary.

M. Meyer (✉) · O. Stiedl
Max Planck Institute for Experimental Medicine, Hermann-Rein Str. 3, 37075 Göttingen, Germany
E-mail: meyer@em.mpg.de
Fax: +49-551-3899249

The arguments that follow are not restricted to heartbeat interval data, but may equally be leveled upon many, if not all, biological time series, e.g., blood pressure, single neuron firing or channel gating dynamics. The characteristic features in observational heartbeat interval time series of normal humans (and other species including rodents), for the purposes of illustration, are compiled in Fig. 1. The left panels (from top to bottom) show an experimental RR-interval time series of a normal subject (upper), a randomly shuffled surrogate of the original time series (middle), and a genuine random data set rescaled to the amplitude of the fluctuations of the original record (lower). A difference in the appearance of the highly irregular, erratic and apparently random behavior is readily apparent upon visual inspection. In traditional linear statistics the measured values are considered as one representative set taken from the entire population having a well-defined arithmetic mean, the sample mean, standard deviation and variance. Hence no differences between the full-length data sets represented in the left panels become apparent, suggesting that the linear properties are the same.

However, the mean and standard deviation calculated for cumulative subepochs of each data set (increasing data length), displayed in the middle-left panels, shows that this impression is wrong. While the statistics for the random sets (middle and lower) rapidly stabilize, those of the original (upper) continue to fluctuate and, with increasing data length, would not converge to constant values. Thus, there is a sizable amount of uncertainty in the estimates of the sample mean and the standard deviation, which would further increase or decrease and never converge if more data were added to the data stream. *These findings suggest that a population mean of the process that generates the data does not exist*. There is thus no single value that can be identified as the "correct" value of the mean. Ultimately, as the amount of data continues to increase the variance continues to increase and becomes infinite.

The *linear* autocorrelation function (C_τ) for increasing lag (τ) is shown in the middle-right panels. Whereas C_τ rapidly decays to zero for the random data sets, the decay for the original is much delayed and follows a power-law indicating the presence of long-time correlations that are absent in the random data. The right panels show the average mutual information I_τ as function of time lag (τ). The information statistic I_τ acts as the *nonlinear* autocorrelation function telling, in a nonlinear way, how the measurements at different times are connected on average over all measurements. This quantity strictly connects the set of observed measurements (s_n) with the same time-lagged set ($s_n+\tau$) and establishes a criterion for their mutual dependence based on the criterion of information connection between the two. If s_n is completely independent of $s_n+\tau$, the amount of information between the two is zero. Hence, the average over all measurements of this information statistic for $\tau=1,2,3,...$ is zero for the random data sets whereas the amount of information gradually declines with increasing τ for the original and s_n and $s_n+\tau$ will eventually become independent for larger τ. $I_{\tau=0}$ is the well-known Shannon entropy of the signal. Stable linear

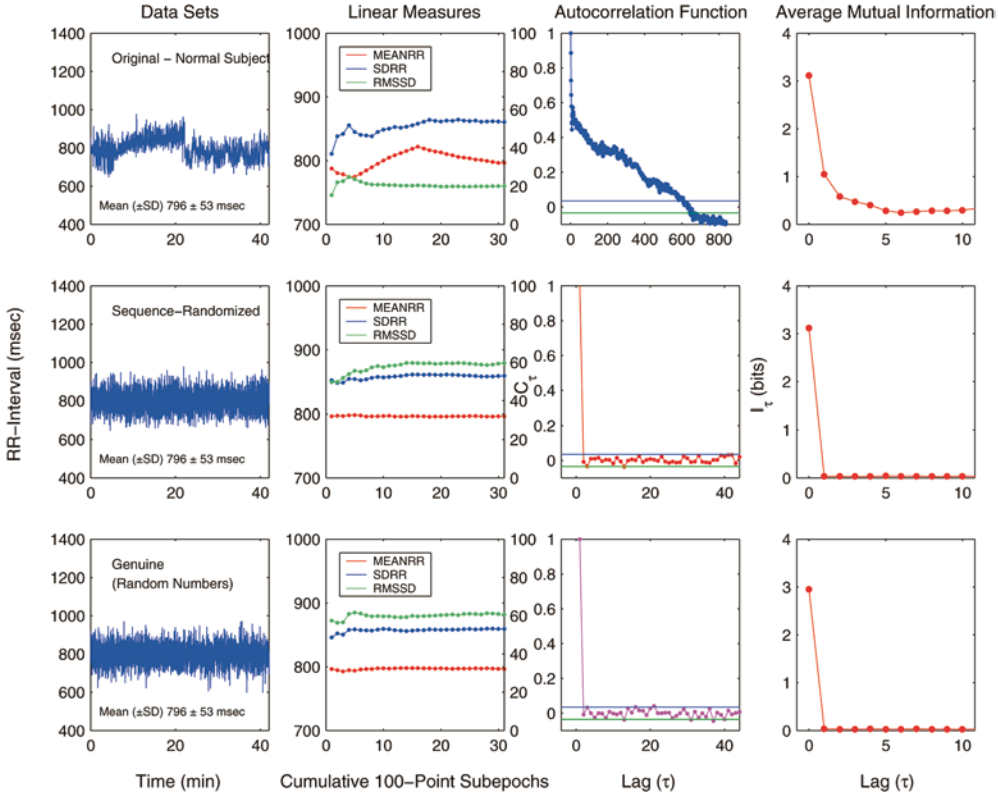

Fig. 1 Linear statistics of experimental and random surrogate data sets. *Left panels*: experimental RR-interval time series (≅40-min recording) of healthy adult human subject (*upper*); randomly shuffled surrogate of experimental time series (*middle*); rescaled genuine random surrogate (*lower*). *Middle-left panels*: RR-interval means (*MEANRR*), standard deviation (*SDRR*) and root-mean square of successive interval differences (*RMSSD*) as a function of accumulated 100-point sub-epochs namely increasing data length. *Middle-right panels*: autocorrelation as a function of increasing lag. Note the shorter *x*-axis scale in *middle* and *lower panels*. *Parallel thin lines* around the *y*-axis origin designate 95% confidence interval for white noise. *Right panels*: average mutual information. See text for details

systems generate zero information, hence selecting information generation as the critical aspect of a nonlinear system assures that the quantities derived (see "Nonlinear time series analysis" and "Multifractal times series analysis") are a property of nonlinear dynamics not shared by linear evolution.

Thus, it becomes evident that, irrespective of the same linear statistics, the dynamics of the original and the random data sets do not share any element in common. The sluggish decay of both the autocorrelation function and the average mutual information observed for the original cardiac time series indicates the existence of *long-range correlations ("memory")* in the data set. Long memory in times series is hard to detect, but has enormous effects on statistical quantities such as standard errors and tests, and hence on the conclusions drawn.

In traditional analysis of irregular biological time series data, e.g., cardiac intervals, it is implicitly assumed that the dynamics is inherently stochastic and produced by a *linear Gaussian random process* that is completely specified by its first and second moments and fully described statistically by the mean, the variance and the autocorrelation function. Hence, if the sample data were indeed representative of a Gaussian distribution, linear statistical analysis focused on the fixed interval associated with the mean would yield traditional variables essentially independent of the interval selected for analysis. Moreover, implicit in this assumption is the idea that the fluctuations around the mean are uncorrelated, structureless random error with normal statistics (normal distribution of probability density function; in fact, much of biology and medicine is definitely not "normal") containing no information about the dynamics.

However, as shown in Fig. 1, an artificial uncorrelated random data set with normal statistics, rescaled to the distribution of the values of the original with the same *linear* properties but no further built-in determinism, shows that the cardiac interval time series has order and structure embedded in the fluctuations that is not present in the uncorrelated time series. The deterministic structure in the cardiac time series results from the fact that future events are causally set by past events ("*memory*"). This underlying complex structure in cardiac interval variability presents a manifestation of *nonlinear* control processes with many interacting components ultimately determining the cardiac rhythm. Hence, the present overview is concerned with nonlinear time series analysis for the detection and quantification of possibly complicated structures in a signal.

Here, we emphasize that many universally accepted linear statistical measures would not adequately describe the complex dynamical properties of heartbeat interval time series, i.e., the correlated structure where each event is statistically dependent on all past ones and results from the ordering of points in time. This is essentially what happens for nonlinear so-called fractal random processes (FRP) and is a consequence of a property of fractals known as self-similarity. We will not review the theory of fractals. Heuristically, a fractal signal produces a self-similar graph; "zooming" (in or out) yields a picture which is similar to the original. The signature of self-similarity implies that: (1) the calculation of mean heartbeat interval or mean heart rate and associated conventional linear statistics for discrimination are meaningless; (2) before any statistical test of dependence is used on heartbeat interval time series, its robustness with respect to infinite variance must be investigated; and (3) novel dimensionless measures may be used to replace well-known but ambiguous linear-stochastic measures that generally encounter the commitment of a type 2 error in the assessment of heartbeat dynamics.

Nonlinear time series analysis

Early studies have attributed the complex dynamics of the cardiac rhythm to be the result of an autonomous low-dimensional deterministically chaotic system but this concept has remained enigmatic (Lefebvre et al. 1993; Yamamoto et al. 1993; Kanters et al. 1994; Sugihara et al. 1996; Poon and Merrill 1997). Physiological systems are typically high-dimensional. For example, heart rate and its variability are modified by variables other than neuroautonomic outflow, such as respiration, arterial blood gases, and circulating hormones. Each of these variables in turn presents the output of dynamics coupled through nonlinear time-delayed feedbacks. Although for truly deterministic systems the entire system's dynamics may be determined from a single measured variable, the feasibility of this approach for noisy biological time series has not been established. It does not seem to be recognized that conventional algorithms for calculation of correlation dimension or Lyapunov exponents have serious limitations in the analysis of physiological data and a convincing demonstration of the utility for high-dimensional systems has not been provided. Nonlinear statistics can however be useful for describing the dynamics of time series even though these systems may not be chaotic in the strict mathematical sense. This can be demonstrated when the value of the statistic changes consistently as some physiological condition changes or by differences between populations in distinctly different physiological states. In many instances the justification for a given statistic is founded on assumptions that may not be appropriate in physiology but nonetheless proves to have physiological significance though the assumptions do not hold.

Recent studies have identified *scale invariance* or *self-affinity* in the fluctuations of cardiac rate which are characterized as *1/f-noise* (strictly, f^{-B}*noise*, with a Fourier spectral density given in terms of the frequency f by the power law f^{-B} and $B \cong 1$) and quantified by a global roughness statistic (Thurner et al. 1988; Peng et al. 1995, 1996; Ivanov et al. 1996, 1998a; Meyer at al. 1998a, 1998b; Amaral et al. 1998). Of particular interest has been the calculation of fractal dimension and scaling properties.

Fractal dimension

The fractal dimension, D, which presents the most important measure of the roughness or irregularity of a time series is calculated from the log-log plot of the relative dispersion, *D*, versus the number of systematically aggregated data points, *n* (Fig. 2, lower left). The relative dispersion is given by the ratio of the standard deviation to the mean. The procedure is to form groups from the original consisting of *m* consecutive data points. The relative dispersion is calculated for each group that is obtained as the aggregates are enlarged to contain increasingly more points (coarse graining). The renormalization group operation of heartbeat intervals beyond their immediate neighborhood yields groups of twos, then groups of threes, then groups of fours and so on. For a simple fractal, *D* decreases as *n* increases and yields a rectilinear line with power-law slope, *b*. D is calculated from the relationship: $D = 1–b$. The straight-line relationship implies that cardiac interbeat dynamics follow an inverse power-law and exhibit scaling which indicates the presence of long-time self-similar correlations extending over hundreds of beats. The serial dependence or "memory" observed in cardiac time series is a reflection of different regulatory mechanisms that, although acting mutually independently on different time scales, are tied together and their effects on heart rate dynamics are interconnected by scaling. This behavior which operates against lawlessness is essentially what is called a *fractal random process* (FRP). In turn, impairment of one individual component of cardiac regulation is expected to influence the other regulatory mechanisms by *interdependence*. The fractal dimension calculated from aggregated dispersion analysis for realizations of sequence-randomized surrogates (D_{SURR}), representing uncorrelated random behavior (white noise), is also displayed in Fig. 2 (lower left). The fractal dimension of normal cardiac interbeat time series is $1.0 > D \ll 1.5$, indicating that the underlying dynamics

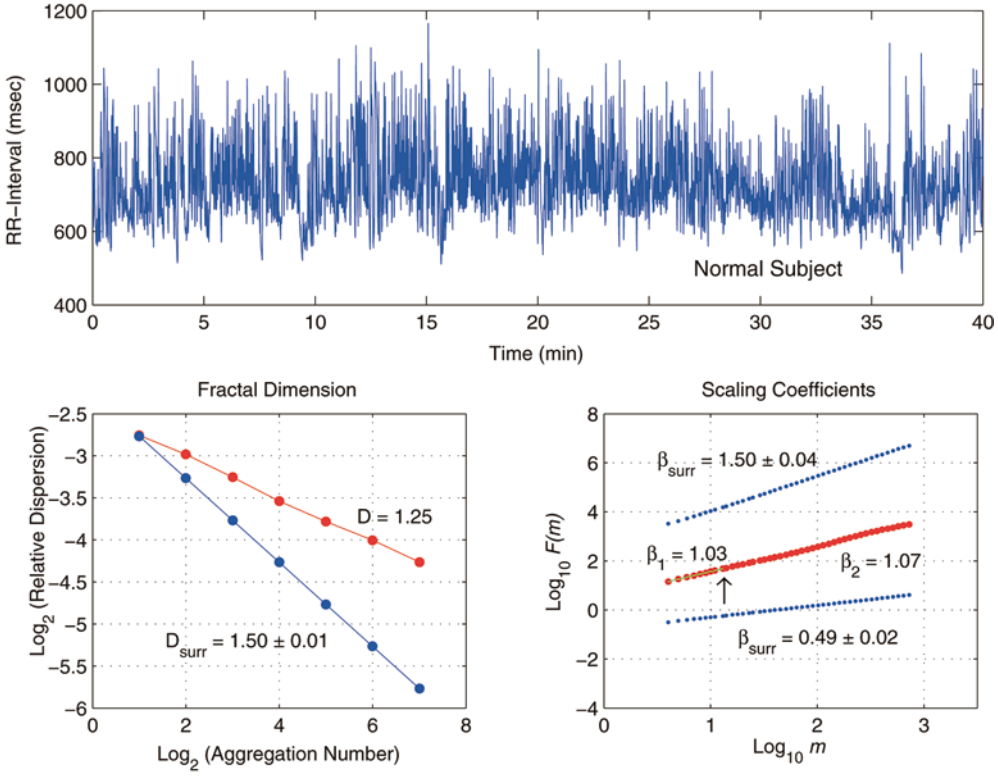

Fig. 2 Non-linear time series analysis. *Upper*: RR-interval time series of healthy subject in supine posture. Fractal dimension – *lower left*: Logarithm, base 2, of relative dispersion (*D*) versus log, base 2, number of aggregated data points (*n*). The *upper line* is the best fit to the data with slope $-0.25 (D_{(n)} \propto n^{-0.25})$ yielding a fractal dimension of $D = 1.25$ for the experimental time series. The *lower line* is the average best fit for an ensemble of 10 realizations of sequence-randomized data sets, i.e., shuffling the original time series data points to random positions in the sequence, with slope –0.50 (0.01) yielding a mean fractal dimension of the surrogates of $D_{surr} = 1.50$ (0.01). The probability that the difference in the slopes between the two lines or fractal dimensions can be explained by a linear, additive, uncorrelated process is $p < 10^{-6}$. Scaling coefficients – *lower right*: Log-log plot of root-mean-square fluctuations [$F_{(m)}$] versus size, namely number of points (*m*) in window. The *points* of *line* in the *middle* follow different regression slopes, β_1 and β_2, separated at a cross-over breakpoint (evident at higher magnification, here indicated by *upward arrow*). The scaling coefficient for short-range correlations in the experimental time series is $\beta_1 = 1.03$; for the long-range correlations it is $\beta_2 = 1.07$. The *lower line* of *points* depicts the average of 10 realizations of sequence-randomized surrogate data sets representing white noise with mean slope $\beta_{surr} = 0.49$ (0.02). The *upper line* of *points* depicts the average of 10 realizations of integrated sequence-randomized surrogate data sets representing Brownian noise (integration of white noise) with mean slope $\beta_{surr} = 1.50$ (0.04). The differences of β_{surr} suggest that the scaling in the experimental time series cannot be explained by white or Brownian noise. See text for details

is different from periodic behavior (D = 1.0) and different from white noise ($D_{SURR} \cong 1.5$), i.e., is fractal.

Scaling coefficients

The calculation of scaling coefficients of a time series by a technique referred to as *Detrended Fluctuation Analysis* (DFA) is derived from principles of random walk theory (Peng et al. 1995; Meyer et al. 1998a; Stiedl and Meyer 2002, 2003). In the DFA analysis the original time series, Y_j, length N, is first integrated. The integrated time series, $Y(k)$, is self-similar if the fluctuations at different observations windows, $F(m)$, scale as a power-law with the window size, m, i.e., the number of cardiac intervals in the window of observation. The root-mean-square fluctuation, $F(m)$, is calculated for all window sizes namely time scales, m:

$$F(m) = \frac{1}{N}\sum_{k=1}^{N}[Y(k) - Y_m(k)]^2 \quad (1)$$

where $Y_m(k)$ denotes the local trend in each window. A linear relationship in the log $F(m)$ versus log m graph indicates that $F(m) \cong m^{\beta}$, where β (slope of the log $F(m)$ versus log m relationship) is the scaling exponent (or self-similarity parameter). In the log-log plot, $F(m)$ typically increases upon recurrent operations with increasing window size m yielding straight-line power-law relationships eventually separated by a cross-over breakpoint (Fig. 2, lower right). The different slopes, β_1 and β_2, are interpreted to reflect the coefficients of distinct ranges of the beat increment: short-range and long-range scaling, respectively. For normal cardiac time series $\beta_1 \cong 1.0$ and $\beta_2 \cong 1.0$. A key issue in the analysis of non-stationary physiological times series data is that fluctuations driven by extrinsic uncorrelated stimuli can be interpreted as a systematic "drift" or "trend" in relation to the frequency of the stimuli and distinguished from the intrinsic correlation properties of the dynamics. These nonstationarities which do not scale the time series are treated by removing the least-squares linear regression trend in each window. For clarity, scaling so interleaves the data that *no* procedure for differencing can remove its effect, i.e., a fractal times series cannot be detrended systematically. Here, the fluctuations scale themselves and the longest and the shortest time scales contributing to the process are tied together so that anything that affects one time scale affects all of them.

Nonstationarity and fractal dynamics

Physiological time series under *free-running* conditions may be visualized as "badly behaved" data originating from nonstationarities driven by uncorrelated extrinsic factors and/or from the intrinsic nonlinear correlated dynamics of a fractal process. In a formal way, the signal generated by a fractal process is nonstationary, i.e., it varies all over as a result of its "built-in" long-range power-law properties and its moments depend on time. A fractal-generating mechanism with fixed components can generate a time series with moments that vary in time. A self-similar fractal process typically produces a time series with long-run dependence of the fluctuations that display the kind of "drift-like" appearance at all time scales. It can be demonstrated that the characteristics of a genuine (computer-generated) self-similar fractal time series demonstrating nonstationarity with "drift-like" appearance at all time scales due to "built-in" long-range power-law correlations ($\beta_{1,2} = 1.0$, $1/f-$noise) display similar fractal dynamics compared to the experimental data of humans. The situation is further complicated by the fact that a fractal process may not be uniscaling or unifractal and hence may not be fully described by a unique fractal dimension or unique scaling coefficients because it may present a time-dependent multiscaling or multifractal process with varying dimensions and scaling properties (see below).

On the other hand, the intrinsic dynamics of a complex nonlinear system may be biased by extrinsic sources, i.e., non-steady state physiological or environmental conditions, that could give rise to highly nonstationary behavior. Although strain-related variations may be physiologically important, their correlation properties would be expected to be related to the stimulus and different from the long-range correlations ("memory") generated by a dynamical system. Unlike the calculation of fractal dimension, D, from the relative dispersion which presumes stationarity of the data stream, the estimation of scaling coefficients, β, does not rely on this assumption. A key issue of the DFA-analysis is that the extrinsic fluctuations from uncorrelated stimuli can be interpreted as "trends" and decomposed (by detrending across time scales) from the intrinsic dynamics of the system itself.

Multifractal time series analysis

Implicit in the calculation of fractal dimension and scaling coefficients (see above) is the assumption that the cardiac interbeat time series is fractionally homogeneous, i.e., *unifractal* or *uniscaling*, and can appropriately be described by a single fractal dimension or scaling coefficient. Further generalization of the analysis beyond the property of uniscaling leads to *multiscaling* or *multifractals* allowing the scaling exponents to depend on time and to be chosen from an infinity of possible distinct values. Multifractals are therefore characterized by a plethora of scaling relations or power-laws with correspondingly many exponents. Multifractals, originally introduced by the seminal papers of Frisch and Parisi (1985), Halsey et al. (1986) and the work of Mandelbrot (1999), exemplify extreme variability and belong to the broad and unified notion of *self-affine*

fractal variation. Evidence for multifractality in human heartbeat dynamics has been suggested earlier (Meyer et al. 1998a, 1998b) and the multifractal formalism based on the Legendre spectrum (see below) has recently been invoked in the analysis of the variability of heart rate (Ivanov et al. 1999).

Multifractal spectrum

Biological signals typically: (1) exhibit significant *long-range dependence* (LRD), but display short-term correlations and scaling behavior inconsistent with strict self-similarity; (2) the scaling behavior of moments is a non-trivial (nonlinear) function of the moment order as the signal is aggregated; (3) the increments in the signal are inherently positive and hence non-Gaussian. Signals with these properties fall naturally into the class of *multifractal processes*. Hence, multifractal analysis retrieves positive measures or distributions exhibiting self-similarity but nonhomogeneous scaling.

The multifractal analysis of irregular but otherwise arbitrary one-dimensional signals is first demonstrated on a classical multifractal signal (trinomial measure, weights: 0.1, 0.3, 0.6; Fig. 3a). The analysis yields a multifractal spectrum [$f(\alpha)$] that may be viewed as a measure of spikiness or global characterization of the singularity structure of the data. It provides information as to which singularities occur in the signal and which are dominant (Falconer 1990; Jaffard 1997; Véhel and Vojak 1998). More precisely, $f(\alpha)$ is a graph where the abscissa represents the *Hölder* or *regularity exponent* (α) in the signal and the ordinate is the fractal co-dimension which measures the extent by which a given singularity is encountered (*coarse-grained multifractal spectrum*). The lower the exponent α, the more irregular is the signal.

Large deviation spectrum

The large deviation spectrum [$f_g(\alpha)$] which is based on the Cramèr Theory of Large Deviations (Holley and Waymire 1992; Véhel and Vojak 1998) is defined as:

$$f_g(\alpha) = \lim_{\varepsilon \to 0} \lim_{n \to \infty} \frac{\ln N_c^n(\alpha)}{-\ln \delta_n}, \tag{2}$$

where

$$N_e^n(\alpha) = \#\left\{\alpha_e^n \middle| \alpha - \alpha_i^n \middle| < \varepsilon\right\}. \tag{3}$$

The function $f_g(\alpha)$ reflects the exponentially decreasing rate of $N_e^n(\alpha)$ which is the number of intervals having a *coarse grain Hölder exponent*, α_i^n, close to a Hölder exponent α up to a precision ϵ when the resolution n approaches ∞. The exponent α_i^n is the logarithm of some quantity measuring the variation e.g., max−min, of the signal in a given interval divided by the logarithm of the interval (Fig. 3b, c). The term δ_n is related to the partition defined by the measure at the resolution n. Hence, the set of α_i^n reflects the scaling behavior of the data at finite resolution. For each resolution n, equispaced intervals are considered. $f_g(\alpha)$ is equal to a Large Deviation

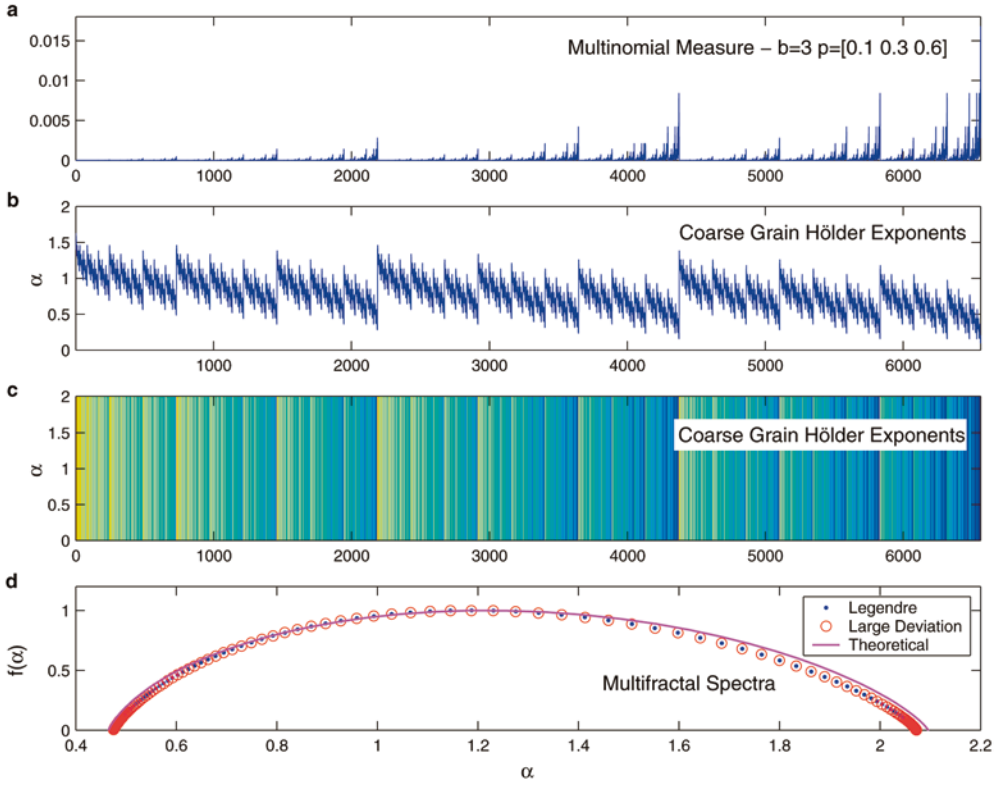

Fig. 3a–d Multifractality of genuine multinomial measure. **a** Time series of multinomial measure (6561 data points). **b** The coarse grain Hölder exponent (α) denotes the range from regularity (high α) to irregularity (low α). The broad range of coarse grain Hölder exponents associated with the signal reflects the complex temporal organization of singularities characterized by the range of irregular fluctuating Hölder exponents. **c** Color coding of **b**. The color spectrum goes from *blue* to *cyan* to *yellow* to *orange* and to *red*. *Blue* indicates small values of α while *yellow-orange* indicates large values of α. **d** The multifractal spectra, $f(\alpha)$ of the Hölder coefficients (α) show smooth concave functions and close agreement of the Legendre and continuous large deviation spectrum with the theoretical spectrum. See text for details

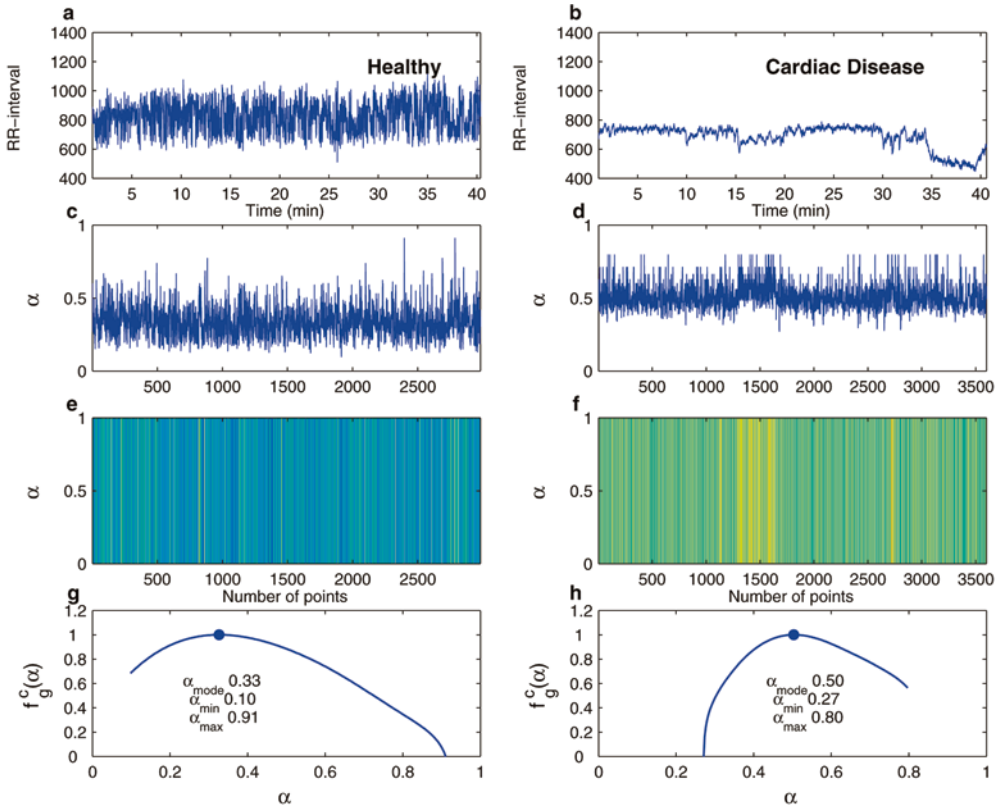

Fig. 4a–h Multifractality in heartbeat interval time series in health (*left panels*) and cardiac disease (*right panels*). Successive heartbeat intervals (ms) as a function of time (≅40 min) from a healthy subject (**a**) and a patient with ischemic heart disease (**b**), both in supine posture. The cardiac time series exhibits wild irregular fluctuations and nonstationary behavior in the healthy subject which is much attenuated in cardiac disease. **c, d** The coarse grain Hölder exponents (α) distributed over the interval [0,1] reflects the heterogeneity that is present in the cardiac time series irrespective of the fact that the subjects were in steady-state resting supine conditions. **e, f** Color coding of **c, d**. **g, h** The continuous large deviation multifractal spectrum, $f_g^c(\alpha)$, of the Hölder coefficients (α) shows a smooth concave function supported by α_{min} to α_{max} with mode, α_{mode} [0.33] for the healthy subject and α_{mode} [0.50] for cardiac patient, indicated by *filled circles*. The extracted parameters, α_{mode}, α_{min}, and α_{max}, respectively, are used to quantify the spectra for the purpose of discrimination and classification of heartbeat interval time series of normal subjects and patients with cardiac disease

Principle (LDP) rate function (Ellis 1985; Riedi 1995; Véhel and Vojak 1998) which measures how frequently or how likely the observed α_i^n deviates from the "expected value" of α. More generally, the multifractal formalism, assessing the singularity spectrum of the function $f_g(\alpha)$, yields information about the statistical behavior of the probability of finding a point with a given Hölder exponent in the signal under changes of resolution.

Continuous large deviation multifractal spectrum

The computation of $f_g(\alpha)$ is based on kernel-density estimation of the coarse grain Hölder exponents α_i^n. The estimator of $f_g(\alpha)$ is optimized for (1) implicit dependency between precision ϵ and resolution n, (2) spatial adaptation of precision ϵ, (3) stable resolution within the range $n_{min} \le n \le n_{max}$, yielding a new definition (Canus et al. 1998), the *continuous large deviation multifractal spectrum*, $f_g^c(\alpha)$ (Fig. 3d). Interval discretization is linearly spaced between α_{min} and α_{max} which are the minimum and maximum values of the coarse grain Hölder exponents. $f_g^c(\alpha)$ yields the large deviations from the "most frequent" singularity exponent and thus displays information about the occurrence of rare events such as bursts (small α). Figure 3d reveals a rich multifractal spectrum indicating that there is "burstiness" in the signal everywhere. Contrary to the more convenient and generally more robust (though at the expense of severe loss of information) Legendre spectrum (Ivanov et al. 1999), $f_e(\alpha)$, which is based on the Legendre transformation of the Rényi exponents $[\tau(q)]$ of the qth moments of the measure and is always shaped like a ∩ (concave and thus continuous, and almost everywhere differentiable), the continuous large deviation multifractal spectrum, $f_g^c(\alpha)$, is superior in that it does not need to be concave and hence is more appropriate in a general setting. It has been demonstrated, that the *partition function* namely moment exponent function $\tau(q)$ and singularity spectra $f(\alpha)$ are mutually related functions and $f(\alpha)$ is the concave hull of $f_g(\alpha)$ (Brown et al. 1992; Véhel and Vojak 1998). For the truly multifractal deterministic measure (Fig. 2a) $f_g(\alpha) = f(\alpha)$, both showing close correspondence with the theoretical multifractal spectrum. The multifractal spectrum addresses the long-range dependence particularly on large scales or

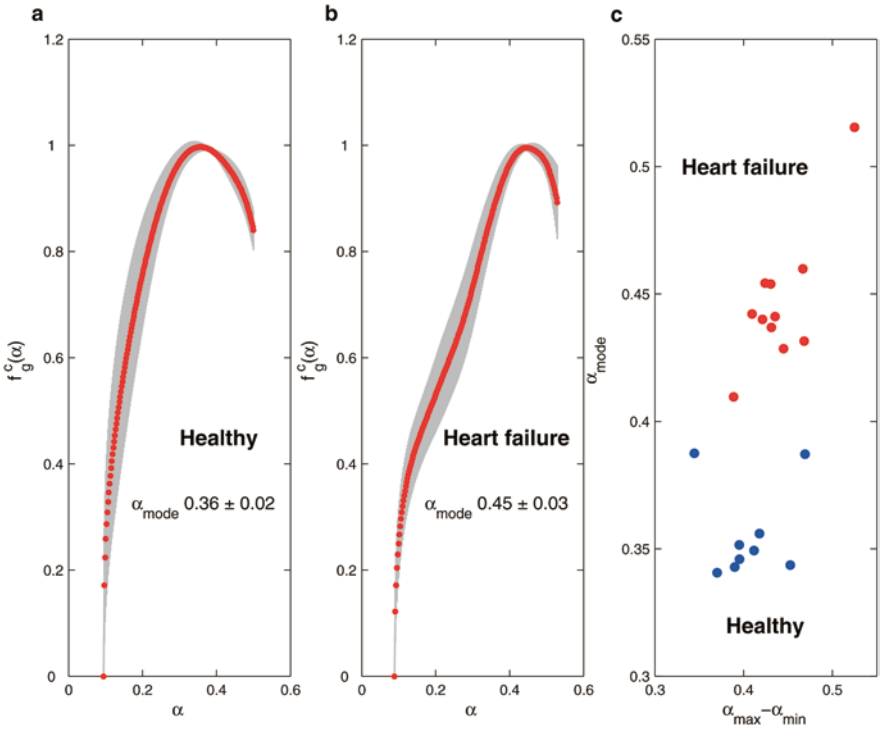

Fig. 5a–c Multifractality in health (**a**) and cardiac disease (**b**). Group averages (SD) of the continuous large deviation multifractal spectrum $f_g^c(\alpha)$ versus Hölder exponents (α) in healthy subjects and patients with congestive heart failure. The broad shape of the multifractal spectra exemplifies multifractal behavior in the cardiac interbeat rhythm which is different between the healthy group and the heart-failure group. The spectra of the cardiac-failure group display a markedly left-sided bimodal shape and shift of α_{mode} towards higher values. **c** Stratification of healthy subjects and patients with congestive heart failure by continuous large deviation multifractal spectrum estimation. Mode of spectrum (α_{mode}) versus degree of multifractality ($\alpha_{max}-\alpha_{min}$) based on full-length 24-h time series records. The multifractal approach clearly discriminates healthy from heart-failure subjects. The results demonstrate that a single quantity, α_{mode}, may be used successfully for discretization of normal subjects and patients with cardiac disease

aggregation levels as well as events such as bursts. Given the strength of a burst with exponent α, the spectrum $f(\alpha)$ indicates how frequently this strength α is encountered. The larger $f(\alpha)$ the more often is α observed.

Experimental data sets

The cardiac interval time series (length $\cong 10^5$ beats) of healthy subjects [$n=9$, 7 males, 2 females; mean age (SD), 33.7 (4.6) years] and patients with congestive heart failure [$n=11$, 9 males, 2 females; mean age (SD), 56.4 (7.2) years] were obtained by 24-h Holter monitoring. The electrocardiographic data base was obtained using a dual-channel ambulatory ECG recorder (Model R6, Custo Med, Munich, Germany) provided with RAM-memory and advanced data compression technology (sampling rate 500 Hz, resolution 2 ms). Additional short-term steady-state episodes (40 min) in healthy control subjects, in patients with nonsustained ventricular tachycardia, and in heart transplant recipients (< 2 years after transplantation) were recorded by a custom-made dual-channel battery-powered miniature ECG recorder amplifier interfaced to a PC by a fiber-optical link (sampling rate 1200 Hz, resolution $\cong$ 0.8 ms).

The digitized ECG was automatically analyzed using an adaptive QRS-template pattern-matching algorithm to obtain a discrete cardiac time series or function, $x(t)=t_{i+1}-t_i$, i.e., the time interval between successive R-wave maxima of the ECG. Ectopic beats or outliers were identified by fitting a third-order autoregressive model to the interbeat interval data points using multiples (3.5) of the interquartile distance as detection threshold and corrected by linear-spline interpolation.

Cardiac dynamics in health and disease

Figure 4 shows the continuous large deviation multifractal spectrum for a healthy adult human subject (left panels) and a patient with ischemic heart disease (right panels). The difference in the dynamics between the two becomes readily apparent by eye, as the human eye is an excellent pattern-recognition device. The quantitative aspect of the difference is reflected in the coarse grain Hölder exponents (Fig. 4c, d) or its colored transformation (Fig. 4e, f) and the disparate shapes of the multifractal spectra (Fig. 4g, h).

For all healthy subjects, the spectrum, $f_g^c(\alpha)$, is a smooth concave function [group mean (SD), α_{mode} 0.36 (0.02); α_{min} 0.09 (0.01); α_{max} 0.50 (0.03)] over a broad range of Hölder exponents α (Fig. 5a). The broad range

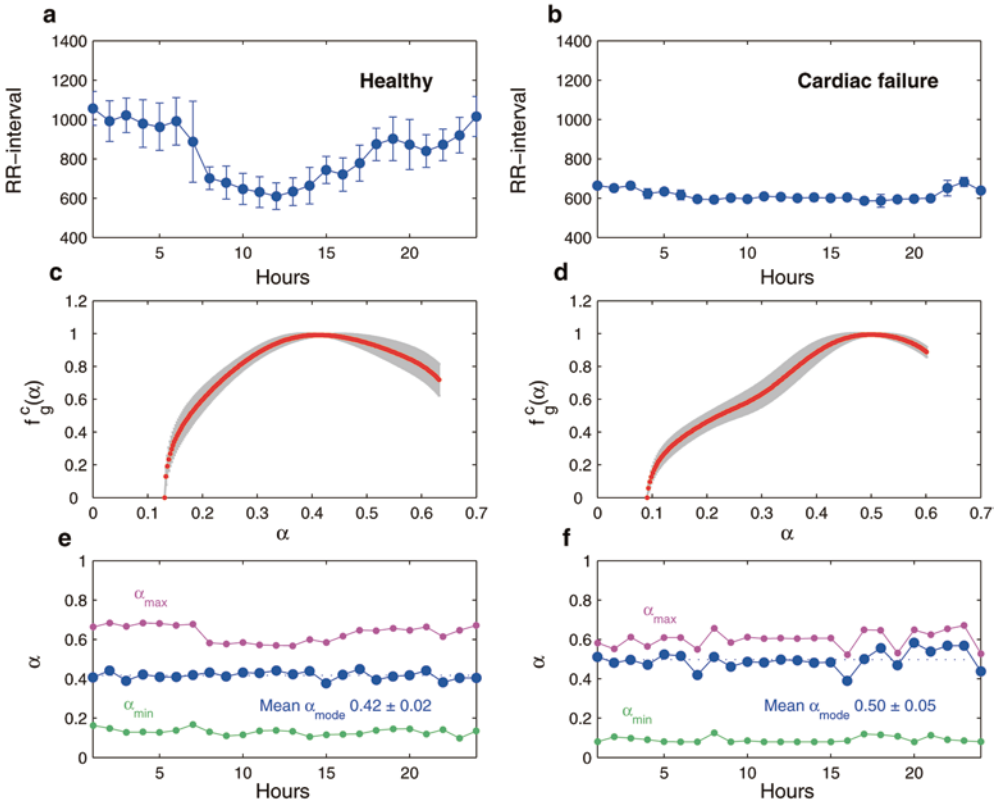

Fig. 6a–f Circadian heart rate dynamics. **a, b** Mean RR-interval (SD) of 1-h sub-epochs versus the time of day in a healthy subject and a patient with congestive heart failure. The heartbeat interval time series of normal subjects exhibit a circadian rhythm with lengthening of RR-intervals (lower heart rate) during night-time episodes which is almost eliminated in chronic cardiac failure. **c, d** Group average (SD) of α versus $f_g^c(\alpha)$ of 1-h sub-epochs. The multifractal spectra display a characteristic difference of shape between health and cardiac failure but exhibit a remarkable stability over a circadian 24-h cycle. **e, f** The mode of the multifractal spectra is lower in normal subjects and higher in cardiac patients but would not undergo systematic circadian-related changes

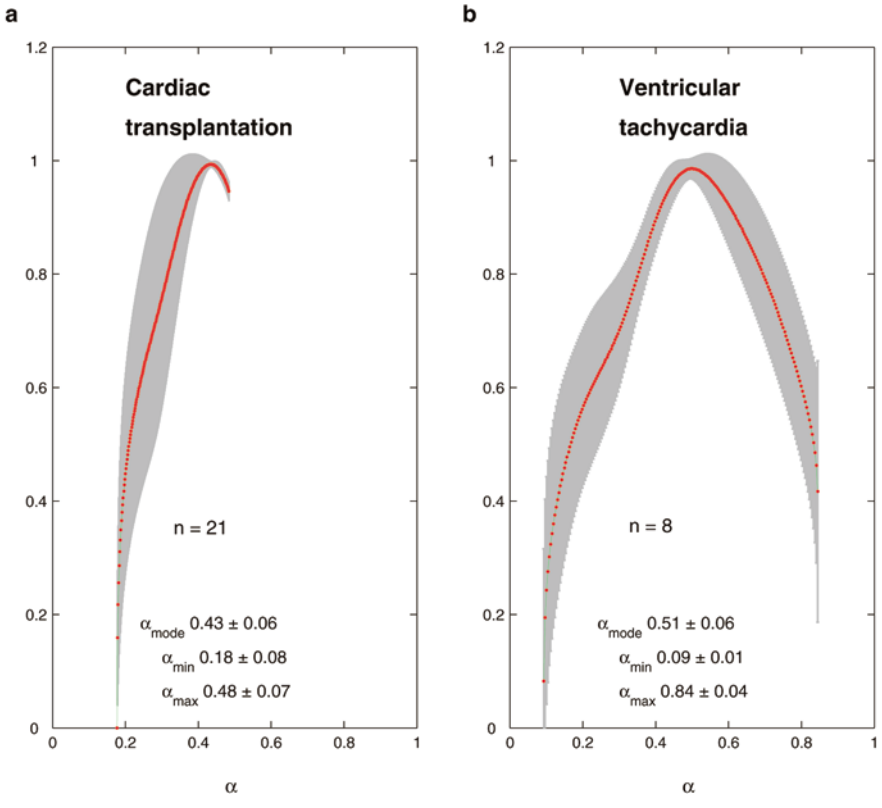

Fig. 7a, b Multifractality and neuroautonomic cardiac control. Multifractal spectra from heart transplant recipients (**a**), and patients with non-sustained ventricular tachycardia (**b**). The different patterns of the multifractal spectra exemplify the importance of neuroautonomic cardiac control in generating the broad-range multifractal spectrum of healthy cardiac dynamics. Cardiac disease is associated with a characteristic pathological shape of the multifractal spectrum

spectrum indicates that heart rate of healthy subjects exhibits multifractal dynamics, i.e., the normal cardiac rhythm displays self-affine multifractal variability. In contrast (Fig. 5b), the spectrum of heart rate dynamics from patients with congestive heart failure consistently displays a marked departure from concavity showing a

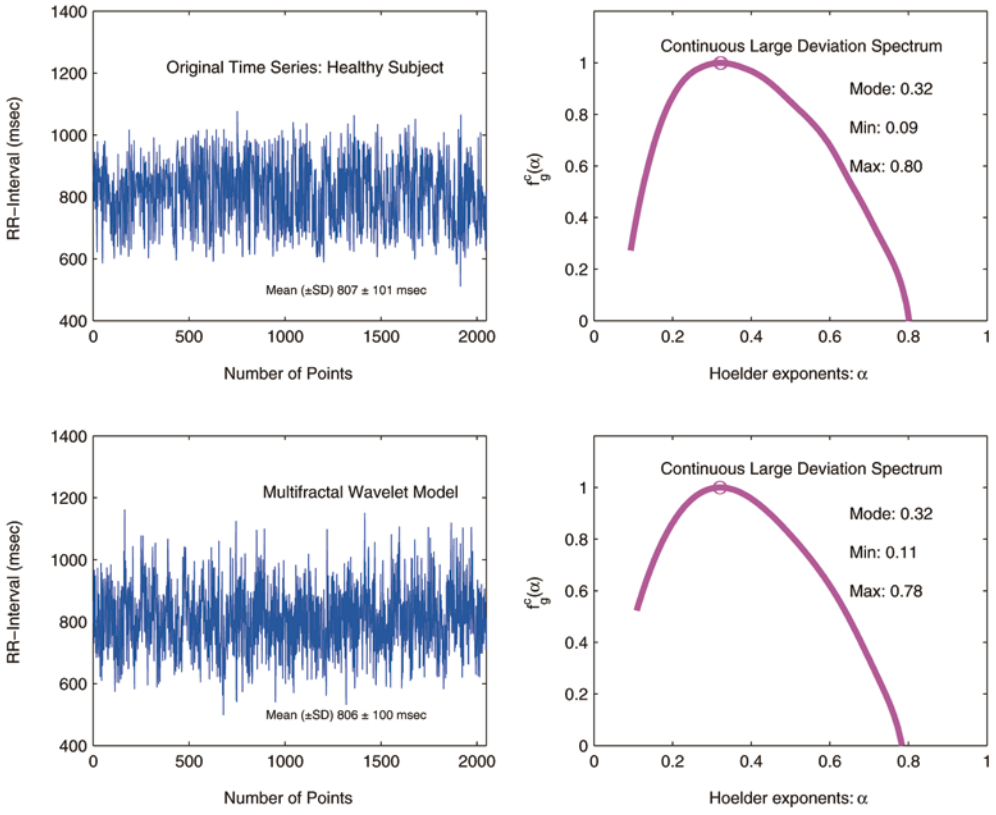

Fig. 8 Modeling of heartbeat interval time series. Original time series of healthy subject (*upper left*) and continuous large deviation multifractal spectrum (*upper right*). Synthesis of cardiac time series by multifractal wavelet model (*lower left*) and continuous large deviation multifractal spectrum (*lower right*). Note the close correspondence of visual appearance and multifractal properties of real and simulated heartbeat interval time series

pronounced trough on the increasing part of the spectrum and α_{mode} is shifted to larger Hölder exponents [group mean (SD), α_{mode} 0.45 (0.03); α_{min} 0.09 (0.02); α_{max} 0.53 (0.04)]. The shift of the α_{mode} to larger values and the "removal" of low singularity strength ($0.1 \leq \alpha \leq 0.4$) render "smoothing" and indicate that the cardiac time series in chronic cardiac disease is more regular while the degree of multifractality given by the α_{max}–α_{min} difference is not materially different between the two groups. The pattern of the spectrum estimate in cardiac patients appears to uncover a superposition of two "basic" spectra reminiscent of those which are observed by synthesis of theoretical multinomial measures, e.g., mixing or sum of two binomial measures. This can be taken as an indication for (at least) two different phenomena underlying perturbation of the dynamics in a pathological condition – congestive heart failure. Less prevalent parasympathetically mediated cardiac control whereby the heart operates in a sympathetically dominated regime signifies the pathophysiology of advanced chronic heart disease.

The calculation of the $f_g^c(\alpha)$ spectrum clearly discriminates healthy subjects from heart-failure patients when based on a single quantity: α_{mode} (Fig. 5c). Further analysis of the data base by randomly selecting subsets of varying data lengths reveals that statistical discrimination of healthy and diseased individuals may be achieved on the basis of any arbitrarily selected segment of 8192 data points which corresponds to an ≅3-h record.

Circadian cardiac dynamics

In order to analyze the circadian stability of the $f_g^c(\alpha)$ spectrum and to assess the impact of *extrinsic* factors such as physical activity, $f_g^c(\alpha)$ was calculated for 1-h sub-epochs of the full-length 24-h data base. While the heart rate of a healthy subject typically shows a circadian rhythm with shorter interbeat intervals (higher heart rates) during day-time episodes and longer intervals (lower heart rates) during night-time epochs (Fig. 6a), cardiac failure patients demonstrate little, if any, circadian changes (Fig. 6b). Indeed, the absence of a circadian rhythm in the clinical setting is interpreted as evidence for chronic heart failure. The multifractal spectrum of the cardiac time series does not undergo appreciable circadian changes in healthy subjects or cardiac patients (Fig. 6c, d) and α_{mode}, α_{max} and α_{min} remain essentially unchanged in the course of the day (Fig. 6e, f). Thus, the physiological mechanisms controlling the dynamics of heart rate appear to be independent of regulatory circadian factors and the form of $f_g^c(\alpha)$ is solely a function of intrinsic factors affecting cardiac activity.

The analysis of short-term data from healthy subjects recorded in steady-state conditions (≅40 min) comparing different postures (supine versus sitting) and the effects of breathing frequency (spontaneous versus paced breathing over a range of 6–48 breaths/min) did not reveal any systematic changes in the $f_g^c(\alpha)$ spectrum (data not shown). These findings along with the absence

of circadian changes suggest that the multifractal spectrum of cardiac dynamics is unlikely to result from extrinsic factors such as physical activity, posture or respiration. This feature of the multifractal spectrum facilitates the comparison of cardiac dynamics across species, e.g., humans versus mice, humans and mice exhibiting identical spectra irrespective of the fact that heart rate in mice is about 8 times higher than in humans (data not shown).

Physiological mechanisms of multifractal variability

The physiological mechanisms underlying the multifractal variability in the cardiac rhythm have not been identified. Intrinsic instability, extrinsic stochastic perturbations and a changing environment act together to produce the intriguing irregular patterns. In healthy subjects, an important mechanism is the control of sinus node activity by the autonomous nervous system. A direct approach as to the significance of autonomic cardiac control for the multifractal dynamics of heart rate is facilitated by studies in recipients of a cardiac transplant (Fig. 7). The data base of heart transplant recipients (<2 years after transplantation) and patients with nonsustained ventricular tachycardia was obtained from 40-min records. The $f_g^c(\alpha)$ spectrum in heart transplant recipients (Fig. 7a) shows a preservation of α_{mode} but cut-off of the upper-range Hölder exponents indicating break-down of multifractality strength which is given by the $\alpha_{\max}$–$\alpha_{\min}$ difference. Thus, the transplanted denervated allograft in transplant recipients which is effectively deprived of its neuroautonomic control is operating over a narrowed multifractal regime. In contrast, patients with episodes of ventricular tachycardia (Fig. 7b) demonstrate enhanced broadening of the spectrum and a bimodal shape similar to that observed in congestive heart failure (cf. Figs. 5b, 6d). These findings emphasize the differential effects of the absence (in cardiac transplantation) or degradation (in ventricular tachycardia) of autonomous nervous system influences on the multifractal spectrum of the cardiac rhythm. However, the precise pathology of neurocardiac control mechanisms that is uncovered by changes in shape of the multifractal spectrum remains to be determined.

Multifractal modeling of heartbeat interval time series

Studying real world physiological data such as heartbeat interval fluctuations is generally restricted to the use of time series analysis techniques aimed at deriving a suitable quantitative statistic in order to discriminate between physiological conditions or populations in physiologically distinct states. Little attention has been given to the modeling of heart rate dynamics. The particular challenge in modeling cardiac traces resides in the "spiky" and "bursty" behavior caused by long-range dependence in the data. A multifractal wavelet model adapted from internet traffic modeling (Riedi et al. 1999) was used for synthesizing coarse-to-fine multiscale positive-valued data with long-range dependence. The model is based on the Haar wavelet transform and a *multiplicative cascade* structure. Starting from a set of training data, the set synthesized by the multifractal wavelet model matches the mean, standard deviation, variance, autocorrelation function and the power spectrum of the original time series. Figure 8 compares the real data of a healthy adult with the result of one realization of the multifractal wavelet model synthesis (left panels). The multifractal continuous large deviation spectra (right panels) reflect the accuracy of the synthesis in terms of the multifractal statistical measure, $f_g^c(\alpha)$. The quality of the matching indicates that the multifractal model convincingly captures and synthesizes the dynamics across large (global behavior) as well as small time scales (rare events, burstiness). The results suggest that the mechanisms interacting in the control of heart rate that operate over time scales from seconds (the parasympathetic nervous system) to hours (renal fluid volume) may exhibit an inherent multiplicative structure.

Concluding remarks

The multifractal properties of heartbeat dynamics elicited by control mechanisms that regulate the cardiac rhythm may be associated with the behavior of dynamical systems typically operating far from equilibrium near a critical point of phase transition (Meneveau and Streenivasan 1987; Ivanov et al. 1998b). Multifractality or multiscaling in cardiac time series signifies the interaction of coupled mixed-feedback systems operating over a wide range of time scales. These properties help provide responsiveness to environmental stimuli (*elasticity*) while preserving a relative insensitivity to errors (*error tolerance*). From a practical point of view, the continuous large deviation multifractal spectrum of heartbeat interval time series is expected to provide a useful diagnostic framework for discretization and classification of patients with cardiac disease and may be applied to other biological time series data.

References

Abarbanel HDI (1996) Analysis of observed chaotic data. Springer-Verlag, Berlin Heidelberg New York

Amaral LAN, Goldberger AL, Ivanov PC, Stanley HE (1998) Scale-independent measures and pathologic cardiac dynamics. Physiol Rev Lett 81:2388–2391

Bassingthwaighte JB, Liebovitch LS, West BJ (1994) Fractal physiology. Oxford University Press, New York

Brown G, Michon G, Peyrière J (1992) On the multifractal analysis of measures. J Stat Phys 66:775–790

Bunde A, Krapp J, Schellnhuber HJ (2002) The science of disasters. Springer-Verlag, Berlin Heidelberg New York

Canus C, Véhel JL, Tricot C (1998) Continuous large deviation multifractal spectrum: definition and estimation. In: Novak MM (ed) Fractals and beyond. World Scientific, Singapore, pp 117–128

Doukhan P, Oppenheim G, Taqqu MS (2003) Theory and applications of long-range dependence. Birkhäuser, Basel
Ellis RS (1985) Entropy, large deviations, and statistical mechanics. Springer-Verlag, Berlin Heidelberg New York
Falconer KJ (1990) Fractal geometry: mathematical foundations and applications. Wiley, New York
Frisch U, Parisi G (1985) Fully developed turbulence and intermittency. In: Ghil M et al. (eds) Turbulence and predictability in geophysical dynamics and climate dynamics. North-Holland, Amsterdam, pp 84–88
Halsey TC, Jensen M, Kadanoff L, Procaccia I, Shraiman B (1986) Fractal measures and their singularities: the characterization of strange sets. Physiol Rev A 33:1141–1151
Holley R, Waymire E (1992) Multifractal dimensions and scaling exponents for strongly bounded random cascades. Ann Appl Prob 2:819–845
Ivanov PC, Rosenblum MG, Peng C-K, Mietus J, Havlin S, Stanley HE, Goldberger AL (1996) Scaling behavior of heartbeat intervals obtained by wavelet-based time-series analysis. Nature 383:323–327
Ivanov PC, Rosenblum MG, Peng C-K, Mietus J, Havlin S, Stanley HE, Goldberger AL (1998a) Scaling and universality of heart rate variability distributions. Physica A 249:587–593
Ivanov PC, Amaral ALN, Goldberger AL, Stanley HE (1998b) Stochastic feedback and the regulation of biological rhythms. Europhysiol Lett 43:363–368
Ivanov PC, Armaral LAN, Goldberger AL, Havlin S, Rosenblum MG, Struzik Z, Stanley HE (1999) Multifractality in human heartbeat dynamics. Nature 399:461–485
Jaffard S (1997) Multifractal formalism for functions: I. Results valid for all functions, II. Self-similar functions. SIAM J Math Anal 28:944–998
Kanters JK, Holstein-Rathlou NH, Agner E (1994) Lack of evidence for low-dimensional chaos in heart rate variability. J Cardiovasc Electrophysiol 5:591–601
Kantz H, Schreiber T (1997) Nonlinear time series analysis. Cambridge University Press, New York
Kaplan DT, Glass L (1995) Understanding nonlinear dynamics. Springer-Verlag, Berlin Heidelberg New York
Lefebvre JH, Goodings DA, Kamath MV, Fallen EL (1993) Predictability of normal heart rhythms and deterministic chaos. Chaos 3:267–276
Mandelbrot BB (1999) Multifractals and 1/f noise. Springer-Verlag, Berlin Heidelberg New York
Meneveau C, Streenivasan KR (1987) Simple multifractal cascade model for fully developed turbulence. Physiol Rev Lett 59:1424–1427
Meyer M, Rahmel A, Marconi C, Grassi B, Skinner JE, Cerretelli P (1998a) Is the heart preadapted to hypoxia? Evidence from fractal dynamics of heartbeat interval fluctuations at high altitude (5050m). Int Physiol Behav Sci 33:9–40
Meyer M, Rahmel A, Marconi C, Grassi B, Cerretelli P, Skinner JE (1998b) Stability of heartbeat interval distributions in chronic high altitude hypoxia. Int Physiol Behav Sci 33:344–362
Peng C-K, Havlin S, Stanley HE, Goldberger AL (1995) Quantification of scaling exponents and crossover phenomena in nonstationary time series. Chaos 5:82–87
Peng C-K, Havlin S, Haussdorff JM, Stanley HE, Goldberger AL (1996) Fractal mechanisms and heart rate dynamics: long-range correlations and their breakdown with disease. J Electrocardiol 28:59–65
Poon C-S, Merrill CK (1997) Decrease of cardiac chaos in congestive heart failure. Nature 389:492–495
Riedi R (1995) An improved multifractal formalism and self-similar measures. J Math Anal Appl 189:462–490
Riedi RH, Crouse MS, Ribeiro VJ, Baraniuk RG (1999) A multifractal wavelet model with application to network traffic. IEEE Trans Signal Proc 45:992–1019
Stiedl O, Meyer M (2002) Fractal dynamics of heart beat interval fluctuations in corticotropin-releasing factor receptor subtype 2 deficient mice. Int Physiol Behav Sci 37:311–345
Stiedl O, Meyer M (2003) Fractal dynamics in circadian cardiac time series of corticotropin-releasing factor subtype-2 deficient mice. J Math Biol 47:169–197
Sugihara G, Allan O, Sobel D, Allan KD (1996) Nonlinear control of heart rate variability in human infants. Proc Natl Acad Sci USA 93:2608–2613
Thurner S, Feurstein MC, Teich MC (1988) Multiresolution wavelet analysis of heartbeat intervals discriminates healthy patients from those with cardiac pathology. Physiol Rev Lett 80:1544–1551
Véhel JL Vojak R (1998) Multifractal analysis of choquet quantities: preliminary results. Adv Appl Math 20:1–43
West BJ (1999) Physiology, promiscuity and prophecy at the millennium: a tale of trails. Word Scientific, Singapore
Yamamoto Y, Hughson RL, Sutton JR, Houston CS, Cymerman A, Fallen EL, Kamath MV (1993) Operation Everest II: an indication of deterministic chaos in human heart rate variability at simulated altitude. Biol Cybern 69:205–212